Preparation and Characterization of Pillared Gallium Aluminum Clays with Enriched Pillars

Xiaozhong Tang,† Wen-Qing Xu,† Yan-Fei Shen,† and Steven L. Suib*,†,‡,§

Department of Chemistry, University of Connecticut, Storrs, Connecticut 06269; Department of Chemical Engineering, University of Connecticut, Storrs, Connecticut 06269; and Institute of Materials Science, University of Connecticut, Storrs, Connecticut 06269

Received June 30, 1994. Revised Manuscript Received November 3, 1994®

Bentolite-H pillared with $GaO_4Al_{12}(OH)_{24}(H_2O)_{12}^{7+}$ ($GaAl_{12}$/B-H) is thermally stable above 700 °C. The cation exchange capacity (CEC) of $GaAl_{12}$ pillared clay is restored by heat treatment in an ammonia atmosphere. This pillared clay is then reintercalated with Ga_{13}, $GaAl_{12}$, and Al_{13} polyoxycations. XRD, surface area, and pore size measurement data show that additional pillars are introduced into the pillared clay. The data for thermal stability of repillared samples indicate improvements in desired properties after reintercalation, especially for $GaAl_{12}$ repillared material. Acidic studies show that the additional pillars introduced by repillaring produce more acid sites on pillared clays. Both Brønsted and Lewis sites are detected on three repillared clays.

Introduction

Clays that have been intercalated with inorganic polyoxycations to replace the exchangeable cations between the silicate layers are a new class of porous materials. Calcination and dehydration lead to the formation of pillared oxides which have a homogeneously distributed bidimensional porous network.[1,2] A great deal of interest has been shown in the preparation of new pillared clays with different sizes of micropores. Their specific properties depend on the type of pillars and on the presence of other metallic ions or complexes. Several cations have been used for pillaring: Al,[4,5] Zr,[6,7] Ti,[8] Si,[9] Cr,[10] Fe,[11] and modified Al-P.[12] Also with mixed pillars Al-Si,[13] Al-Zr,[4] and Al-La,[14] a significant improvement in thermal stability of pillared clays has been made.[15]

Recently, pillaring clays with gallium has been drawing more and more attention because of the similarity of Ga and Al in chemistry.[16-20,24] The preparation of mixed Al-Ga pillared clays with high thermal stability has been attempted.[16-20,24] Three pillared clays with Ga_{13}, $GaAl_{12}$, and Al_{13} polyoxycations have been synthesized in a previous study.[21] The pillared clay with $GaAl_{12}$ shows good two-dimensional structure and high thermal stability. The incentive here is to further exploit possibilities of making mixed pillared clays with high thermal stability. Modified synthetic routes were employed, seeking to intercalate more pillars in interlamellar spacings for high thermal stability. Different thermal stabilities and acidities were observed for the three repillared clays.

Experimental Section

A. Synthesis. The clay used in these experiments was bentolite-H (i.e., B-H) which is a white bentonite produced from native, colloidal aluminum silicate by ECC America Inc. It is 68.1% SiO_2, 13.5% Al_2O_3, 2.9% MgO, 0.7% Fe_2O_3, 0.9% CaO, 3.5% Na_2O, 0.1% K_2O, and 0.2% TiO_2. X-ray diffraction patterns for this material can be found elsewhere.[31] The clay was pretreated to obtain homoionic Na bentonite, and the <2 μm fraction was used for pillaring. The cation-exchange capacity of the treated bentonite, determined by the Kjeldahl method on the NH_4^+-exchanged form, was 75 mequiv/100 g of clay.

The pillaring agents of $AlO_4Al_{12}(OH)_{24}(H_2O)_{12}^{7+}$, $GaO_4Ga_{12}(OH)_{24}(H_2O)_{12}^{7+}$, and $GaO_4Al_{12}(OH)_{24}(H_2O)_{12}^{7+}$ polyoxy-

† Department of Chemistry.
‡ Department of Chemical Engineering.
§ Institute of Materials Science.
* To whom correspondence should be addressed at the Department of Chemistry.
® Abstract published in *Advance ACS Abstracts,* December 15, 1994.

(1) Vaughan, D. E. W.; Lussier, R. J. *Proc. Int. Conf. Zeol., 5th* **1980**, 94.
(2) (a) Vaughan, D. E. W.; Lussier, R. J.; Magee, J. S. U.S. Patent 4176090, 1979. (b) Vaughan, D. E. W.; Lussier, R. J.; Magee, J. S. U.S. Patent 4,271,043, 1981.
(3) Figueras, F. *Catal. Rev.* **1988**, *30*, 457.
(4) Occelli, M. L.; Finseth, D. H. *J. Catal.* **1986**, *99*, 316.
(5) Jones, S. L. *Catal. Today* **1988**, *2*, 209.
(6) Bartley, G. J. *J. Catal. Today* **1988**, *2*, 233.
(7) Farfan-Torres, E. M.; Grange, P. *J. Chim. Phys.* **1990**, *87*, 1545.
(8) Yamanaka, S.; Nishihara, T.; Hottori, M.; Suzuki, Y. *Mater. Chem. Phys.* **1987**, *17*, 87.
(9) Endo, T.; Mortland, M. M.; Pinnavaia, T. J. *Clays Clay Miner.* **1981**, *29*, 153.
(10) Carrado, K. A.; Suib, S. L.; Skoularikis, N. D.; Coughlin, R. W. *Inorg. Chem.* **1986**, *25*, 4217.
(11) Occelli, M. L.; Stencel, J. M.; Suib, S. L. *J. Mol. Catal.* **1991**, *64*, 221.
(12) Shen, Y. F.; Ko, A. N.; Grange, P. *Appl. Catal.* **1990**, *67*, 93.
(13) Sterte, J.; Shabtai, J. *Clays Clay Miner.* **1987**, *35*, 429.
(14) Sterte, J. *Preparation of Catalysts*; Elsevier Science Publishers B. V.: Amsterdam, 1991; Vol. V, p 301.
(15) Sterte, J. *Clays Clay Min.* **1991**, *39*, 167.
(16) Bradley, S. M.; Kydd, R. A.; Yamdagni, R. *J. Chem. Soc., Dalton Trans.* **1990**, 2653.
(17) Bradley, S. M.; Kydd, R. A.; Yamdagni, R. *J. Chem. Soc., Dalton Trans.* **1990**, *413*.
(18) Bradley, S. M.; Kydd, R. A.; Yamdagni, R. *Magn. Reson. Chem.* **1990**, *28*, 764.
(19) Bradley, S. M.; Kydd, R. A. *Catal. Lett.* **1991**, *8*, 185.
(20) Gonzalez, F.; Pesquera, C. *Inorg. Chem.* **1992**, *31*, 727.
(21) Tang, X.; Xu, W.; Shen, Y.; Suib, S. *Synthesis and Characterization of Gallium Pillard Clay Catalysts for Butane Aromatization*, ACS Sym. Chicago, Aug **1993**.
(22) Barrett, E. P.; Joyner, L. G.; Halenda, P. P. *J. Am. Chem. Soc.* **1951**, *73*, 373.
(23) Horvath, G.; Kawazoe, K. *J. Chem. Eng. Jpn.* **1983**, *15*, 470.
(24) (a) Bradley, S. M.; Kydd, R. A. *Catal. Lett.* **1990**, *8*, 15. (b) Bradley, S. M.; Kydd, R. A. *J. Catal.* **1993**, *141*, 239. (c) Bradley, S. M.; Kydd, R. A. *J. Catal.* **1993**, *142*, 448. (d) Bradley, S. M.; Kydd, R. A.; Yamdagni, R. In: *Proc. Mat. Res. Soc.*, Fall 1990, Symposium S, Synthesis and Properties of New Catalysts: Utilization of Novel Materials, Components and Synthetic Techniques; pp 69-72.

0897-4756/95/2807-0102$09.00/0

cations (i.e., Al_{13}, Ga_{13}, and $GaAl_{12}$) were prepared by a modified literature procedure.[16] About 80 mL of 0.5 N NaOH solution was slowly dropped into (about 0.5 mL/min) a solution of $AlCl_3$, $GaCl_3$, or into a mixture of $GaCl_3$ and $AlCl_3$ (Ga^{3+}:Al^{3+} = 1:12) respectively under vigorous stirring to give an OH^-:M^{3+} ratio of 2.0. The mixed solutions then were diluted to an M^{3+} concentration of 0.1 M $GaAl_{12}$ and Al_{13} pillaring agents were aged at 70 °C for 8 h, but the Ga_{13} agent was used for pillaring immediately after it was made because it can dissociate into smaller species in a short period of time.[16]

To enhance cation-exchange capacity CEC of the pillared clay for further reintercalation, the $GaAl_{12}$/B−H intercalated clay was heated at a desired temperature in an atmosphere of ammonia as shown by Vaughan et al.[2b] To choose ideal conditions, the sample was heated at different temperatures in the range 200−500 °C, in a stream of He or NH_3 for 2 h. To remove the ammonia adsorbed on acidic sites, the ammonia treated samples were treated in a stream of He at the same temperature for 2 h. The cation-exchange capacities (CEC) of the treated pillared clays were determined by the Kjeldahl method and were compared. A temperature of 300 °C was chosen as the ideal temperature for treatment with NH_3.

The pillared clay $GaAl_{12}$/B−H was used for repillaring because it has the best crystallinity and the highest thermal stability among the three pillared clays. $GaAl_{12}$/B-H pillared clay (2 g) which was treated in an ammonia stream at 300 °C, was resuspended in 100 mL of distilled deionized water (DDW). The pillaring agents [Ga_{13}, $GaAl_{12}$, or Al_{13} (10 mmol of M^{3+}/g of clay)] were slowly dropped into a vigorously stirred $GaAl_{12}$/B−H clay suspension containing 2 g of clay, respectively. After being mixed, the suspension was kept stirring at room temperature overnight and then transferred to a dialysis tube for 5 day dialysis with changing DDW every day. After dialysis, the clay sample was separated by centrifuging the suspension and washed with DDW until Cl^- could not be detected by precipitation with $AgNO_3$. Finally, the repillared clay samples were freeze-dried.

For comparison purposes a gallium ion-exchanged $GaAl_{12}$/B−H material was prepared by ion-exchanging 1 g of the $GaAl_{12}$ pillared clay with 100 mL of a 0.1 M $GaCl_3$ solution for 8 h. After exchange, the Ga^{3+}/$GaAl_{12}$−B−H material was filtered, washed with DDW, and tested with $AgNO_3$ solution for residual Cl^-. Samples were then freeze−dried.

B. Characterization. *1. NMR Measurements.* ^{71}Ga NMR spectra of $GaAl_{12}$ pillaring agent were acquired on a Varian Unity Plus Model 400 (21C-VXR) spectrometer at room temperature (21 °C). The chemical shifts are referred to $Ga(H_2O)_6^{3+}$ solution. Acquisition time was 0.3 s, with a pulse time of 8 μs and a relaxation delay of 3 s.

2. X-ray Diffraction. X-ray diffraction studies were performed by using a Scintag XRD-2000 X-ray diffractometer with Cu Kα radiation with a current of 40 mA and a voltage of 45 kV. Dry powder samples were used for XRD measurements.

3. Chemical Analysis. Chemical analysis was carried out by inductively coupled plasma emission spectrometer with a Perkin-Elmer P-40 ICP. Samples were dissolved with mixtures of concentrated HF, HNO_3, and HCl. Standard solutions were used for calibration to determine elemental concentrations.

4. Surface Area and Pore-Size Distribution. Surface areas were measured by adsorption of N_2 at −196 °C in an Omnisorp-100CX analyzer after outgassing of the samples at 150 °C for 6 h. The BET equation was used to determine the surface area. Microporosity was studied by analyzing the N_2 adsorption isotherms up to relative pressure of 0.3. Micropore volumes and micropore size distributions were obtained by means of *T*-plot analysis and HK method;[22] Meso- and macroporosities were studied by analyzing the N_2 desorption isotherms from relative pressures of 0.2 to 1. The BJH method was used to determine the volume of meso- and macropores.[23]

5. Thermal Analysis. Thermogravimetric analysis (TGA) and differential thermogravimetric analysis (DTG) were carried out on a Perkin-Elmer 7 series thermal analysis system in N_2 atmosphere with a flow rate of 20 mL/min and a heating rate of 10 °C/min.

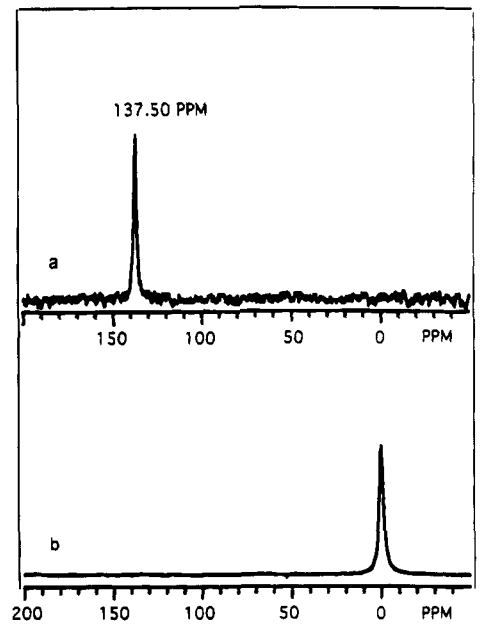

Figure 1. ^{71}Ga NMR spectra of (a) $[GaO_4Al_{12}(OH)_{24}(H_2O)_{12}]^{7+}$ pillaring agent and (b) $Ga(H_2O)_6^{3+}$.

6. Fourier Transform Infrared Spectroscopy. FTIR spectra were collected on a Mattson Galaxy spectrometer with 2-cm^{-1} resolution by using self-supporting wafers and a triglycine sulfate detector. Pyridine chemisorption experiments were done on self-supporting wafers of pillared clays in a home-built *in situ* cell. Pillared clay pellets were first evacuated at 150 °C for 4 h at 10^{-5} Torr and then exposed to pyridine for 15 min. FTIR spectra were then recorded after pellets were evacuated for 2 h at 150, 275, 400, and 500 °C respectively.

7. Temperature-Programmed Desorption. TPD experiments were done on a home-built system consisting of a gas chromatography detector, a tube furnace, a temperature programmer, an integrator, and a quartz reactor. A temperature program rate of 15 °C/min was used in the experiments. Samples were first dehydrated in He at 500 °C for 1 h and then cooled to 100 °C in He; then ammonia was sorbed at 100 °C and physisorbed ammonia was removed with flowing He at 100 °C for 1 h. Temperature programming in He gas was then carried out.

Results

A. NMR. The ^{71}Ga NMR spectra (Figure 1) show that the six-coordinate gallium species, $Ga(H_2O)_6^{3+}$, has a peak at 0 ppm. The $GaAl_{12}$ polyoxycation, which was made as a pillaring agent, shows no peak at 0 ppm but a peak at 137 ppm, indicating a tetrahedrally coordinated gallium nucleus. This peak position is in agreement with the peak position reported for the structure of $GaO_4Al_{12}(OH)_{24}(H_2O)_{12}^{7+}$.[24] As the NMR results suggest, the $GaO_4Al_{12}(OH)_{24}(H_2O)_{12}^{7+}$ polyoxycation is formed in the pillaring agent. A reviewer has suggested that it is unlikely that all of the Ga may be observed by NMR due to exchange and/or quadrupolar effects which may mask the true situation.

B. CEC Results. Figure 2 shows a change of CEC for $GaAl_{12}$/B−H pillared clay (which was selected as a mother-pillared clay due to high thermal stability) after being treated at different temperatures in either He or NH_3 atmospheres. In both atmospheres, the CEC show the same trends as temperature increases. The CEC reaches a maximum at 300 °C and goes down at higher temperatures. After being treated in an ammonia atmosphere, the pillared clay has higher CEC values

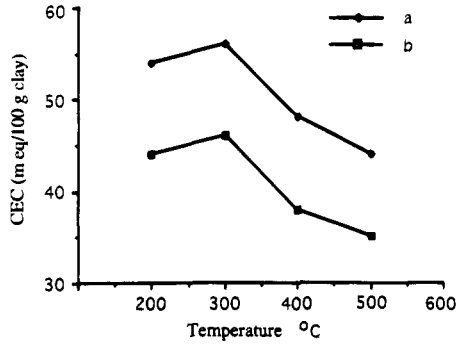

Figure 2. CEC of $GaAl_{12}$/B−H pillared clay treated in different atmospheres: (a) in NH_3; (b) in helium.

than in helium. About 85% of the CEC of the original unpillared bentonite is retained as the pillared clay is treated in an ammonia atmosphere at 300 °C if one takes into account weight changes after pillaring. However, only about 50% of the original CEC is retained in helium for treatment at the same temperature (300 °C). Due to results of CEC measurements, $GaAl_{12}$/B−H pillared clay treated at 300 °C in a stream of ammonia was chosen as a mother pillared clay for repillaring studies.

C. Structural Data. XRD patterns for $GaAl_{12}$/B−H are shown in Figure 3a and summarised in Table 1. The XRD data of Table 1 and Figure 3b−d show that the *d* (001) spacing for ammonia-treated $GaAl_{12}$/B−H pillared clay is 18.8 Å. After it has been reintercalated with Ga_{13}, $GaAl_{12}$, and Al_{13} polyoxycations, the *d* spacing increases slightly to 19.2 and 18.9 Å for Ga_{13}/$GaAl_{12}$/B−H and $GaAl_{12}$/$GaAl_{12}$/B−H, respectively. For Al_{13}/$GaAl_{12}$/B−H, the *d* spacing does not change. Of the three repillared clays, the two repillared with $GaAl_{12}$ and Ga_{13} polyoxycations have more intense and sharper (001) peaks than the one pillared with Al_{13}, indicating a more ordered structure for Ga_{13} and $GaAl_{12}$ materials (see Figure 3).

After the samples have been treated in air for 2 h at 500 °C (Table 1) the *d* spacing decreases slightly to 18.8 and 18.1 Å, respectively, for Ga_{13}/$GaAl_{12}$/B−H and Al_{13}/$GaAl_{12}$/B−H. There is no change in *d* spacing for $GaAl_{12}$/$GaAl_{12}$/B−H. The relative intensities of all three peaks decrease, especially in the case of Al_{13}/$GaAl_{12}$/B−H. From XRD patterns (Figure 3A) it is seen that repillared clays such as $GaAl_{12}$/$GaAl_{12}$/B−H still have very intense and sharp (001) peaks at 500 °C, while Al_{13}/$GaAl_{12}$/B−H has a much weaker and broader (001) peak. Ga_{13}/$GaAl_{12}$/B−H is in between, having a fairly intense and sharp (001) peak. Compared to the XRD pattern for $GaAl_{12}$/B−H without repillaring, these three repillared clays have higher *d* spacings at this temperature (500 °C).

The *d* spacings continue to decrease as samples are further heated to 700 °C. The (001) peaks decrease to 18.0, 18.0, and 17.0 Å for Ga_{13}/$GaAl_{12}$/B−H, $GaAl_{12}$/$GaAl_{12}$/B−H, and Al_{13}/$GaAl_{12}$/B−H repillared clays, respectively. However, at this temperature the *d* spacings of the repillared clays with $GaAl_{12}$ and Ga_{13} polyoxycations have higher values and relative intensities than $GaAl_{12}$/B−H, indicating the higher thermal stability of the repillared clays. The Al_{13}/$GaAl_{12}$/B−H sample has about the same *d* spacing as that of $GaAl_{12}$/B−H heated at 700 °C. XRD patterns show that the (001) peak for Al_{13}/$GaAl_{12}$/B−H becomes very weak and broad at 700 °C, showing no improvement of thermal stability after Al_{13} repillaring.

Table 1. Basal Spacings and Relative Intensities of $GaAl_{12}$/B−H and Repillared Clays

	d (001) Å			intensity		
	150 °C	500 °C	700 °C	150 °C	500 °C	700 °C
$GaAl_{12}$/B−H	18.8	17.6	17.1	306	263	203
repillared with Ga_{13}^{7+}	19.2	18.8	18.0	476	274	214
repillared with $GaAl_{12}^{7+}$	18.9	18.9	18.0	470	429	365
repillared with Al_{13}^{7+}	18.8	18.1	17.0	387	178	146

Table 2. Surface Area and Pore Size Distribution of Repillared Clays

	S_{BET} (m^2/g)			V_{micro} (mL/g)		
	150 °C	500 °C	700 °C	150 °C	500 °C	700 °C
$GaAl_{12}$/B−H	290	269	198	0.076	0.076	0.049
repillared with Ga_{13}	220	207	184	0.053	0.049	0.037
repillared with $GaAl_{12}$	214	215	204	0.048	0.053	0.046
repillared with Al_{13}	182	161	121	0.034	0.033	0.024

D. Surface Areas and Pore Size Distributions. The surface areas and the micropore volumes of $GaAl_{12}$/B−H and the three repillared clays are summarized in Table 2. $GaAl_{12}$/B−H has a surface area of 290 m^2/g after being evacuated at 150 °C to remove physisorbed H_2O. Surface areas for repillared samples decrease to 220, 214, and 182 m^2/g for Ga_{13}/$GaAl_{12}$/B−H, $GaAl_{12}$/$GaAl_{12}$/B−H, and Al_{13}/$GaAl_{12}$/B−H, respectively. This is also the case for micropore volumes, whose diameters are smaller than 20 Å, and which are supposed to be created by intercalation of polyoxycations. Among the three repillared clays, Ga_{13}/$GaAl_{12}$/B−H and $GaAl_{12}$/$GaAl_{12}$/B−H have values of 0.052 and 0.049 mL/g, while Al_{13}/$GaAl_{12}$/B−H has a much smaller value of 0.034 mL/g.

The heat treatment at 500 °C does not significantly change the surface areas and micropore volumes of Ga_{13}/$GaAl_{12}$/B−H, $GaAl_{12}$/$GaAl_{12}$/B−H, and Al_{13}/$GaAl_{12}$/B−H. However, there is a slight increase in micropore volume from 0.049 to 0.053 mL/gm for $GaAl_{12}$/$GaAl_{12}$/B−H due to heat treatment at 500 °C.

After the samples are thermally treated at 700 °C, apparent decreases in surface areas and micropore volumes are observed for Ga_{13}/$GaAl_{12}$/B−H and Al_{13}/$GaAl_{12}$/B−H, which have lost 35 and 20 m^2/g of surface area and 0.015 and 0.01 mL/g of micropore volume, respectively from that at 150 °C. However, $GaAl_{12}$/$GaAl_{12}$/B−H has not lost much of its surface area or micropore volume and still has the highest value of the three repillared clays. Compared to $GaAl_{12}$/B−H, $GaAl_{12}$/$GaAl_{12}$/B−H has about the same surface area and micropore volume at this temperature.

E. Bulk Analysis. Table 3 summarizes the amounts of Al and Ga in $GaAl_{12}$/B−H, repillared clays, and Ga^{3+} ion-exchanged $GaAl_{12}$/B−H samples. The numbers of pillars in 1 g of pillared clay have been calculated by assuming that one pillar is formed from one polyoxycation intercalated in the interlayer spacing. The amount of Al present in B−H is subtracted from the total [Al] determined from bulk analysis. The Al/Ga ratio for the $GaAl_{12}$/$GaAl_{12}$/B−H was found to be 12.0. The Al/Ga ratio for the $GaAl_{12}$/B−H material before pillaring was also found to be 12.0. These were determined in relation to the amount of Si and the original Si/Al ratio of B−H. It is noticed that after repillaring,

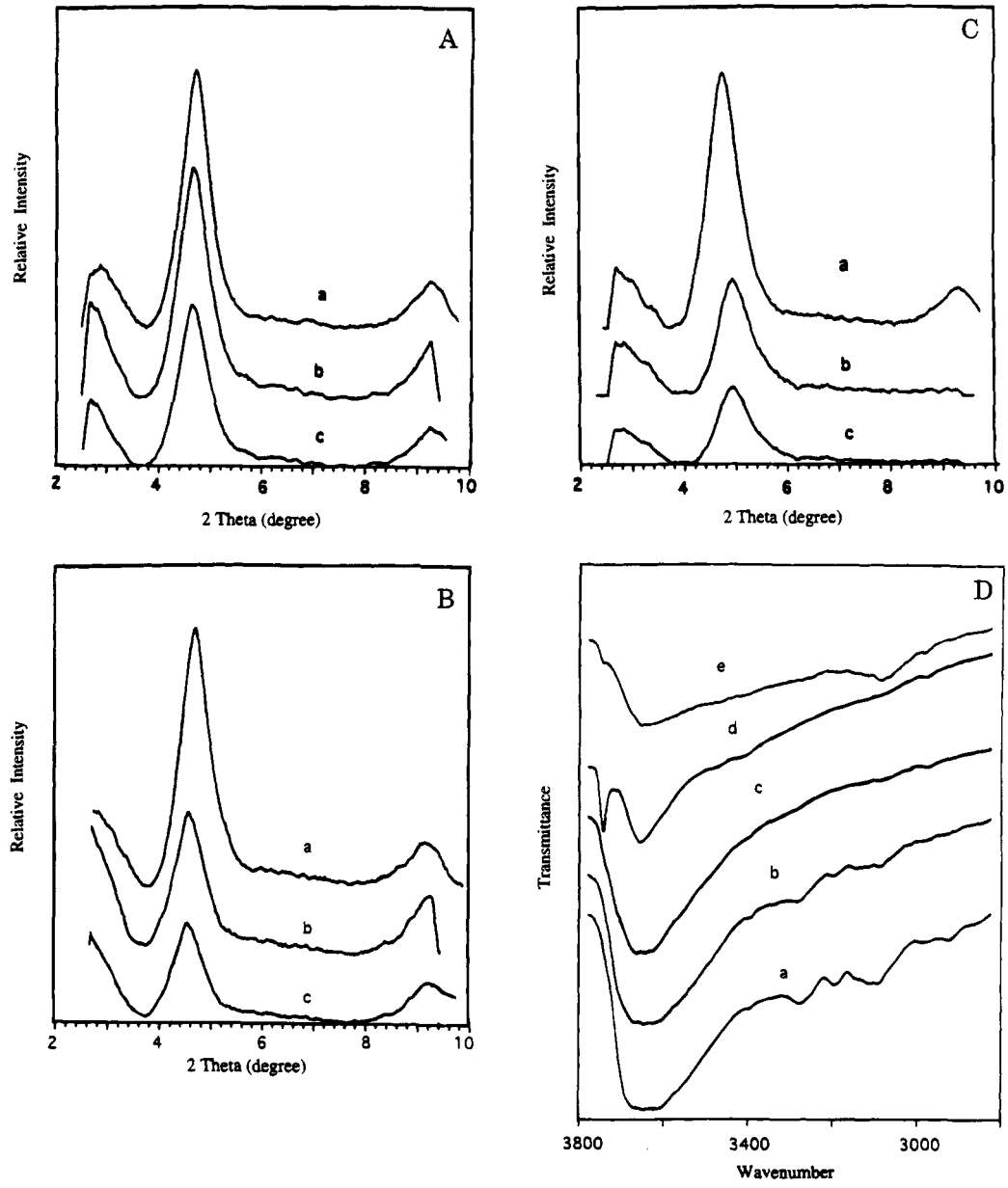

Figure 3. (A) X-ray diffraction of $GaAl_{12}$/B−H clay: (a) 25 °C; (b) 500 °C; (c) 700 °C. (B) X-ray diffraction of repillared clay, $GaAl_{12}/GaAl_{12}$/B−H: (a) 25 °C; (b) 500 °C; (c) 700 °C. (C) X-ray diffraction of repillared clay, $Ga_{13}/GaAl_{12}$/B−H: (a) 25 °C; (b) 500 °C; (c) 700 °C. (D) X-ray diffraction of repillared clay, $Al_{13}/GaAl_{12}$/B−H: (a) 25 °C; (b) 500 °C; (c) 700 °C.

Table 3. Chemical Analysis and Number of Pillars per Gram of Clay

clay	$GaAl_{12}$/B−H	Ga^{3+} $GaAl_{12}$/B−H	Ga_{13}^{7+} $GaAl_{12}$/B−H	$GaAl_{12}^{7+}$ $GaAl_{12}$/B−H	Al_{13}^{7+} $GaAl_{12}$/B−H
mg of Ga/g	15.8	32.7	74.7	19.7	13.0
mg of Al/g	101	98.4	93.9	116	114
no. of pillars/g of clay	1.36×10^{20}	1.36×10^{20}	1.75×10^{20}	1.70×10^{20}	1.63×10^{20}

pillars increase from 1.36×10^{20} to 1.75×10^{20}, 1.70×10^{20}, and 1.63×10^{20}/g for $Ga_{13}/GaAl_{12}$/B−H, $GaAl_{12}/GaAl_{12}$/B−H, and $Al_{13}/GaAl_{12}$/B−H, respectively.

F. Thermal Analysis. Thermogravimetric analyses of repillared clay samples are presented in Figure 4. Two major steps for weight loss for each sample are observed. The first one occurs up to 150 °C with a deep slope. This step is assigned to loss of surface physisorbed water and loosely coordinated water. The second step occurs between 150−600 °C with a shallow slope corresponding to the dehydroxylation of polyoxycation pillars in between silicate layers. Above 600 °C the weight losses are due to the dehydration of silicate layers of the clay.

Table 4 shows the weight percentage lost by repillared clay samples in different temperature ranges. It is noticed that the sample repillared with $GaAl_{12}$ polyoxycation has lost the largest amount of weight among all samples, which is 16% up to 900 °C. In the range 150−600 °C, weight loss is 8.2% for $GaAl_{12}/GaAl_{12}$/B−H which is >7.2% for $Al_{13}/GaAl_{12}$/B−H and which is >7.2% for $Ga_{13}/GaAl_{12}$/B−H.

Figure 5 shows DSC curves of three repillared clays and an ion-exchanged clay sample. From the first derivatives, it is seen that endotherms occur at 200 °C for both $Ga_{13}/GaAl_{12}$/B−H and $Ga^{3+}/GaAl_{12}$/B−H. For $GaAl_{12}/GaAl_{12}$/B−H and $Al_{13}/GaAl_{12}$/B−H, the endotherm is at 150 °C and is smaller than for the other

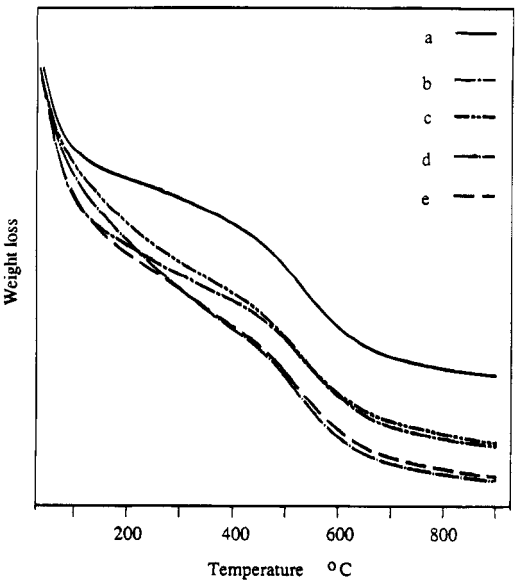

Figure 4. TGA curves of (a) $GaAl_{12}$/B−H, (b) Ga^{3+}/$GaAl_{12}$/B−H, (c) Ga_{13}/$GaAl_{12}$/B−H, (d) $GaAl_{12}$/$GaAl_{12}$/B−H, and (e) Al_{13}/$GaAl_{12}$/B−H.

Table 4. Weight Loss (%) of Repillared Clays in Different Temperature Ranges

clay	25−150 °C	150−600 °C	25−900 °C
Ga_{13}/$GaAl_{12}$/B−H	7.2	6.5	14.6
$GaAl_{12}$/$GaAl_{12}$/B−H	8.2	6.9	16.0
Al_{13}/$GaAl_{12}$/B−H	7.2	7.6	15.8
$GaAl_{12}$/B−H[a]	5.8	6.1	12.8

[a] Treated at 300 °C in ammonia.

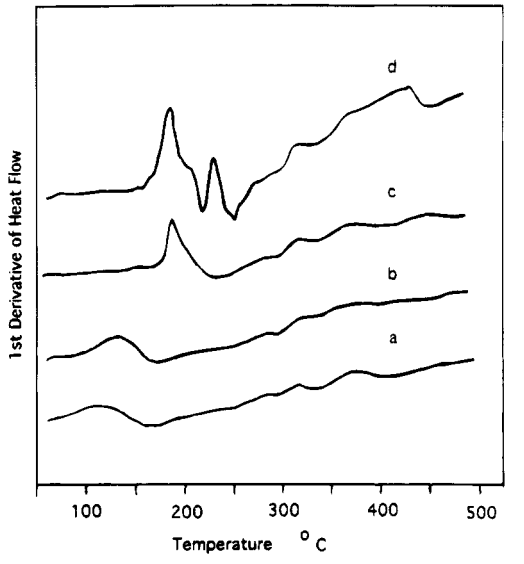

Figure 5. DSC curves of (a) $GaAl_{12}$/$GaAl_{12}$/B−H, (b) Al_{13}/$GaAl_{12}$/B−H, (c) Ga_{13}/$GaAl_{12}$/B−H, and (d) Ga^{3+}/$GaAl_{12}$/B−H.

samples. These peaks are assigned to heats of desorption for physisorbed or loosely coordinated water molecules.

G. Pyridine FTIR and Ammonia TPD. Figure 6 presents the Fourier transform infrared spectra for repillared clays and an Ga^{3+} ion-exchanged clay, which have been evacuated at 150 °C, exposed to pyridine vapor, followed by evacuation at 150 °C to remove physisorbed pyridine, and then evacuated at different temperatures. At 150 °C, the four samples show similar spectra, bands at 1454 and 1620 cm^{-1} are assigned to Lewis acid sites, due to pyridine coordinated via its nitrogen lone-pair electrons to an empty p-orbital, while bands at 1545 cm^{-1} are assigned to Brønsted acid sites, indicating formation of the pyridinium ion by reaction with surface protons. The strong bands at 1490 cm^{-1} are due to both Lewis and Brønsted acid sites. At 275 °C, the bands at 1545 cm^{-1} for Al_{13}/$GaAl_{12}$/B−H and $GaAl_{12}$/$GaAl_{12}$/B−H shrink dramatically. However, the same bands for Ga_{13}/$GaAl_{12}$/B−H and Ga^{3+}/$GaAl_{12}$/B−H are still apparently seen, indicating stronger Brønsted acid sites on these two samples. Bands of pyridine adsorbed on the Lewis acid site are fairly strong. As temperature increases to 400 °C and further to 550 °C, adsorbed pyridine bands for all samples decrease significantly, but the bands for both acid sites can still be observed. On Ga_{13}/$GaAl_{12}$/B−H and Ga^{3+}/$GaAl_{12}$/B−H a small band at 1598 cm^{-1} appears at 400 °C, and becomes more obvious at 550 °C. On $GaAl_{12}$/$GaAl_{12}$/B−H and Al_{13}/$GaAl_{12}$/B−H, these bands are not observed. This band is in the wavenumber range for Lewis acid sites and could be due to gallium species. After the samples are cooled at room temperature, reexposure to pyridine vapor, and evacuated at 150 °C, bands for pyridine adsorption on Lewis and Brønsted acid sites become stronger, especially on $GaAl_{12}$/$GaAl_{12}$/B−H and Ga_{13}/$GaAl_{12}$/B−H.

Figure 7 presents the Fourier transform infrared spectra in the OH^- stretching region. Different spectra are observed for the different samples. At 150 °C, Ga_{13}/$GaAl_{12}$/B−H and Ga^{3+}/$GaAl_{12}$/B−H show a broad free OH^- band centered about 3653 cm^{-1} due to isolated Al−OH or Si−OH groups. As temperature is increased to 550 °C, a weaker peak at about 3737 cm^{-1} is seen; this is due to surface Al−OH Brønsted species, which readily react with pyridine at low temperature.[25] This peak disappears as pyridine is readsorbed at 150 °C. On $GaAl_{12}$/$GaAl_{12}$/B−H the peak is about 3737 cm^{-1} appears at lower temperatures, i.e., 275 °C. On Al_{13}/$GaAl_{12}$/B−H, the same peak even exists at 150 °C. In the range of 3300−2800 cm^{-1}, peaks which are due to the aromatic C−H stretch of adsorbed pyridine can be seen on all the samples, and as evacuation temperature increases they become weaker.

The ammonia desorption data for repillared and Ga^{3+} ion-exchanged clays are presented in Figure 8. Only one peak is observed for each sample and the temperature maximum for ammonia desorption is at about 172 °C for all samples. All peaks tail, indicating a slow loss of acid sites. The amounts of ammonia desorbed from samples up to 500 °C depend on the types of pillars. It is seen that the acid sites on $GaAl_{12}$/$GaAl_{12}$/B−H have been increased significantly from 331 ($GaAl_{12}$/B−H) to 418 μmol/g after repillaring. Al_{13}/$GaAl_{12}$/B−H (355 μmol/g) and Ga_{13}/$GaAl_{12}$/B−H (332 μmol/g) show a small increase in acid sites. However, note that some acid sites are lost after ion-exchange of Ga^{3+}/$GaAl_{12}$/B−H, (262 μmol/g).

Discussion

A. Cation-Exchange Capacity. Thermal treatment converts the polyoxycation $GaAl_{12}$ into Ga_2O_3 and

(25) Zhao, D.; Yang, Y.; Gua, X. *Inorg. Chem.* **1992**, *31*, 4727.

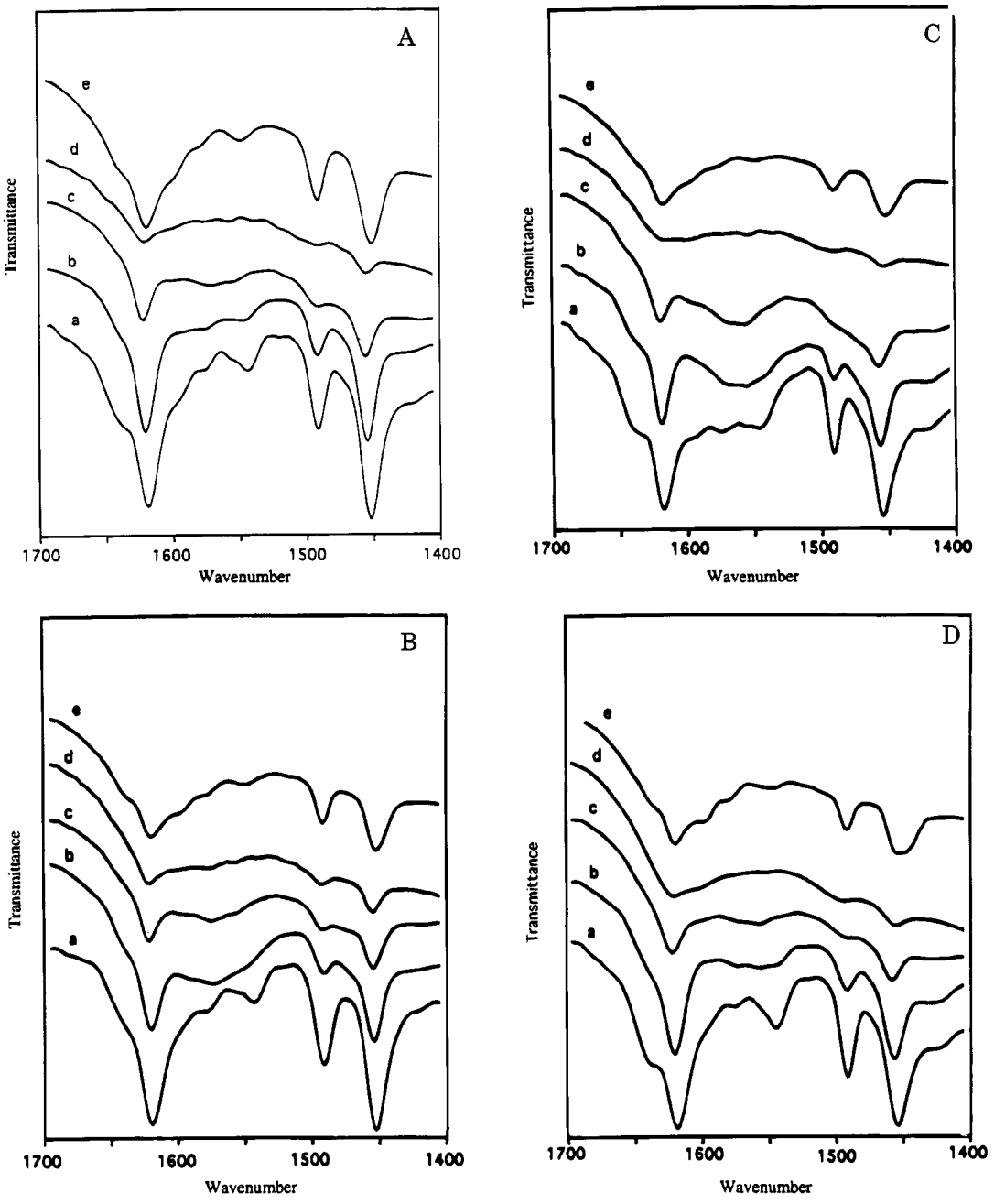

Figure 6. (A) IR spectra of adsorbed pyridine on repillared clay, $GaAl_{12}/GaAl_{12}/B-H$, evacuated at (a) 150 °C, (b) 275 °C, (c) 400 °C, (d) 550 °C, and (e) exposed to pyridine again and evacuated at 150 °C. (B) IR spectra of adsorbed pyridine on repillared clay, $Al_{13}/GaAl_{12}/B-H$, evacuated at (a) 150 °C, (b) 275 °C, (c) 400 °C, (d) 550 °C, and (e) exposed to pyridine again and evacuated at 150 °C. (C) IR spectra of adsorbed pyridine on repillared clay, $Ga_{13}/GaAl_{12}/B-H$, evacuated at (a) 150 °C, (b) 275 °C, (c) 400 °C, (d) 550 °C, and (e) exposed to pyridine again and evacuated at 150 °C. (D) IR spectra of adsorbed pyridine on Ga^{3+}-exchanged pillared clay, $Ga^{3+}/GaAl_{12}/B-H$, evacuated at (a) 150 °C, (b) 275 °C, (c) 400 °C, (d) 550 °C, and (e) exposed to pyridine again and evacuated at 150 °C.

Al_2O_3, which can be represented as follows:

$$[GaO_4Al_{12}(OH)_{24}(H_2O)_{12}]^{7+} \rightarrow 0.5Ga_2O_3 + 6Al_2O_3 + 7H^+ + 20.5H_2O \quad (1)$$

This indicates that, theoretically, after heat treatment, the pillared clay should have the same cation-exchange capacity (CEC) as that of the original clay due to protons that are generated assuming no weight change. However, the migration of H^+ and other small cations to vacant sites or lower charged centers of octahedral and tetrahedral symmetry at high temperature[26,27] can decrease the CEC of pillared clays significantly. This is also observed from the data for $GaAl_{12}/B-H$ pillared clay heated in a He atmosphere in Figure 2 that only less than half of the original CEC is obtained at 300 °C. Above the temperature, the CEC drops even more dramatically. The migration of small cations plays an important role in this process. Pillared clays exhibit larger CECs after thermal treatment in an ammonia vapor than in helium. An explanation for this could be that NH_3, which has Brønsted and Lewis basicity,

(26) Russell, J. D.; Frazer, A. R. *Clays Clay Min.* **1971**, *13*, 55.
(27) Yariv, S.; Heller-Kallai, L. *Clays Clay Miner.* **1973**, *29*, 199.

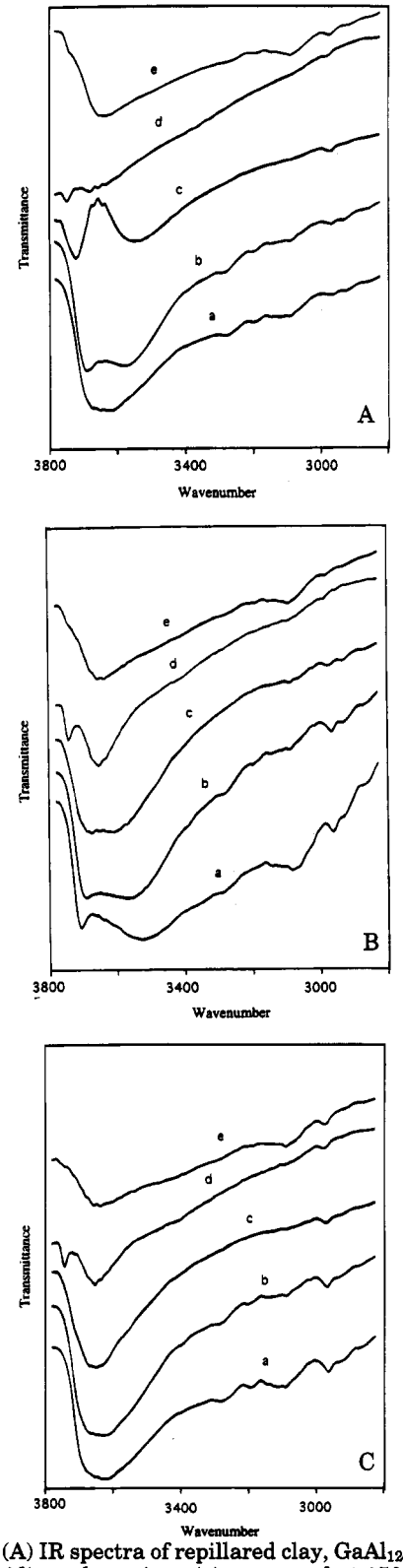

Figure 7. (A) IR spectra of repillared clay, $GaAl_{12}/GaAl_{12}/B-H$, with pyridine adsorption: (a) evacuated at 150 °C, (b) 275 °C, (c) 400 °C, (d) 500 °C, and (e) evacuated at 150 °C after readsorption of pyridine. (B) IR spectra of repillared clay, $Al_{13}/GaAl_{12}/B-H$, with pyridine adsorption: (a) evacuated at 150 °C, (b) 275 °C, (c) 400 °C, (d) 500 °C, and (e) evacuated at 150 °C after readsorption of pyridine. (C) IR spectra of repillared clay, $Ga_{13}/GaAl_{12}/B-H$, with pyridine adsorption: (a) evacuated at 150 °C, (b) 275 °C, (c) 400 °C, (d) 500 °C, and (e) evacuated at 150 °C after readsorption of pyridine. (D) IR spectra of Ga^{3+}-exchanged pillared clay, $Ga^{3+}/GaAl_{12}/B-H$, with pyridine adsorption (a) evacuated at 150 °C, (b) 275 °C, (c) 400 °C, 500 °C, and (e) evacuated at 150 °C after readsorption of pyridine.

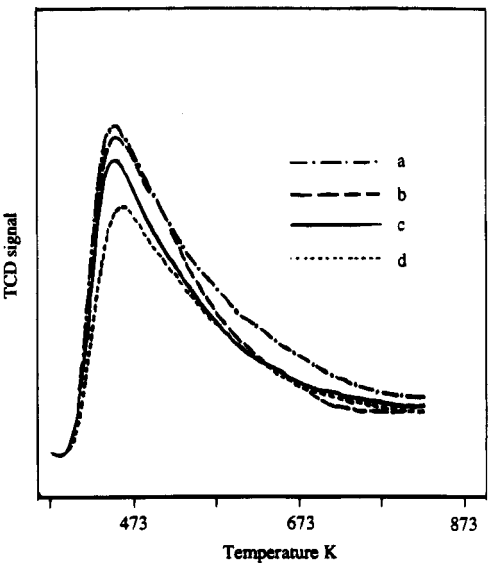

Figure 8. Ammonia TPD of (a) $GaAl_{12}/GaAl_{12}/B-H$, (b) $Al_{13}/GaAl_{12}/B-H$, (c) $Ga_{13}/GaAl_{12}/B-H$, and (d) $Ga^{3+}/GaAl_{12}/B-H$.

attracts protons or other cations on the surface of the clay due to migration into the framework of the clay. Also, the existence of a base could accelerate the forward reaction of eq 1, which generates oxide pillars and exchangeable cations. Similar cases were reported when pillared clays were treated with steam or in solution.[28]

Since it was concluded in the previous part of this study[21] and elsewhere[19] that $GaAl_{12}/B-H$ has the highest thermal stability among the three pillared clays, the pillared $GaAl_{12}/B-H$ clay heated in ammonia vapor at 300 °C was chosen as a mother pillared clay for repillaring studies. CEC data also support this choice.

B. Composition and Structure of Repillared Clays. For reintercalation, the exchangeable cations which are generated by means of heat treatment in NH_3 vapor are replaced by polyoxycations. It is known that the selectivity of cation exchange in silicates depends on both the charge and size of cations.[29,30] The selectivity is higher for highly charged cations. In this case, the polyoxycations have a 7+ charge, which is much higher than 1+ or 2+ charges of the small exchangeable cations. However, the rate of exchange is expected to be lower for bulkier species, like polyoxycations in this case. To overcome this problem, a high concentration of polyoxycations is important. In this study the amount of polyoxycations for 1 g of clay is 30 mmol/g of clay, and this overwhelmingly controls the amount of exchangeable cations in clay interlayers which is less

(28) Kikuchi, E.; Seki, H.; Matsuda, In: Poncelet, G., Jacobs, P. A., Grange, P., Delmon, R., Eds. *Preparation of Catalysts*; Elsevier Science Publishers, B. V. Amsterdam, 1991; Vol. V.
(29) Breck, D. W. *Zeolite Molecular Sieves*; Wiley-Interscience: New York, 1974.
(30) Sherman, J. In *Zeolites: Science and Technology*; Ribieiro, F. R., Rodrigues, A. E., Rollman, L. D., Naccache, C., Eds. Nato ASI Ser. 80; Maritinus Nijhoff: The Hague, 1984; p 583.
(31) (a) Suib, S. L.; Carrado, K. A. *Inorg. Chem.* **1985**, *24*, 863. (b) Suib, S. L.; Tanguay, J. M.; Occelli, M. L. *J. Am. Soc.* **1986**, *108*, 6972. (c) Carrado, K. A.; Suib, S. L.; Skoularikis, N. D.; Coughlin, R. W. *Inorg. Chem.* **1986**, *25*, 4217. (d) Skoularikis, N. D.; Coughlin, R. W.; Carrado, K. A.; Kostapapas, A.; Suib, S. L. *Solid State Ionics* **1986**, *22*, 117. (e) Skoularikis, N. D.; Coughlin, R. W.; Carrado, K. A.; Suib, S. L. *Appl. Catal.* **1988**, *39*, 61. (f) Shi, C.; Rusling, J. F.; Wang, Z.; Willis, A. M.; Winiecki, A. M.; Suib, S. L. *Langmuir* **1989**, *5*, 650. (g) Occelli, M. L.; Stencel, J. M.; Suib, S. L. *Stud. Surf. Sci. Catal.* **1991**, *60*, 353. (h) Occelli, M. L.; Stencel, J. M.; Suib, S. L. *J. Mol. Catal.* **1991**, *64*, 221.

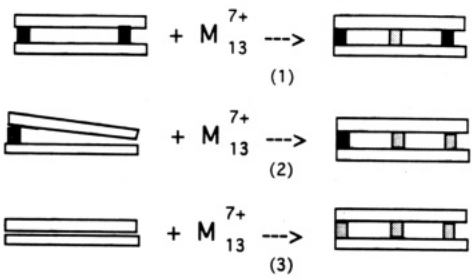

Figure 9. Three possibilities for the reintercalation process.

than 0.56 μmol for 1 g of clay. The long exchange time (over 5 days) enables polyoxycations to compete with smaller cations and diffuse into the micropores generated in the first pillaring process. Also, dialysis enables small cations exchanged from the pillared clays to be removed from the system, so polyoxycations have more chance to diffuse into pores. The height of pillars of $GaAl_{12}$/B−H pillared clay treated at 300 °C in ammonia is about 9.3 Å, which is about the size of polyoxycations; so it is possible for polyoxycations to diffuse into the micropores.

As compared to the (001) peak for $GaAl_{12}$/B−H shown in Figure 3a, the sharper and more intense (001) peaks of repillared clays in XRD patterns of Figure 3b−d reveal that the pillared clay has been successfully reintercalated with $GaAl_{12}$, Ga_{13}, and Al_{13} polyoxycations, respectively. A slight increase in d spacing after repillaring can be explained by the three scenarios of Figure 9.

Since the d spacing obtained from powder XRD is an average value for all small particles, all three possibilities can make contributions to an increase in d spacing. The increase is so small that possibility 3 is not significant. The sequence of d spacings of repillared clays is Ga_{13}/$GaAl_{12}$/B−H > $GaAl_{12}$/GaA_{12}/B−H > Al_{13}/$GaAl_{12}$/B−H, which is the same as the sequence of sizes of the three polyoxycations used for reintercalation. This result also supports the conclusion of successful reintercalation.

Results of surface area and pore size distribution measurements support our conclusions as well. Small decreases in surface areas and micropore volumes after reintercalation are due to more pillars being generated in interlayer spacings which block N_2 molecules from reaching the internal surface. Among the three repillared clays, Al_{13}/$GaAl_{12}$/B−H has the lowest degree of reintercalation. This is the same trend we observed from the first intercalation,[21] in which Al_{13}/B−H had the smallest d spacing, the lowest intensity of the (001) peak, the smallest surface area, and the smallest micropore volume. This may be attributed to dissociation of the Al_{13} polyoxycation into smaller oligomeric species.

Calculating the amount of pillars in 1 g of clay indicates that after reintercalation, about 30% more pillars are introduced into the pillared clay with $GaAl_{12}$ and Ga_{13} polyoxycations. However, with Al_{13} polyoxycations, only about 20% more are introduced. The CEC of ammonia treated $GaAl_{12}$/B−H pillared clay is 56 mequiv/100 g of clay. If all polyoxycations were replaced by polyoxycations whose charge is 7+, a total of 0.48×10^{20} new pillars would be introduced. Nevertheless, in this research only 0.39×10^{20}, 0.34×10^{20}, and 0.27×10^{20} new pillars are introduced for Ga_{13}, $GaAl_{12}$, and Al_{13} pillars, respectively. Diffusion problems may play an important role in this case, because the bulky polyoxycations may find it difficult to reach the very center part of the particle. In addition, the different results for amounts of Ga content obtained from ICP data for Ga_{13}/$GaAl_{12}$/B−H repillared clay suggest that most newly introduced pillars are not in the very center of the pillared clay particles. X-ray photoelectron spectroscopy data have also been used to verify this suggestion.

The results of XRD, surface area, and micropore volume measurements for Ga^{3+} ion-exchanged pillared clay show no obvious change from that of $GaAl_{12}$/B−H. This is reasonable, since Ga^{3+} cations are so much smaller than polyoxycations that they only replace exchangeable cations, and do not effect the structure of $GaAl_{12}$/B−H pillared clays.

C. Thermal Stability. The silicate sheet of clays is remarkably stable, and the collapse of the pillared clay is mainly attributed to the sintering of pillars. Two factors appear to control the thermal stability, the density of the pillars, and the distribution of pillars within interlayer spacings.

By comparing the results of XRD, surface area, and micropore volumes of $GaAl_{12}$/B−H pillared clay to those of repillared clays, it is easily seen that the thermal stability of the pillared structure is increased after repillaring, especially in the cases of $GaAl_{12}$/$GaAl_{12}$/B−H and Ga_{13}/$GaAl_{12}$/B−H. This increase may be due to the contribution of extra pillars introduced by repillaring.

The different thermal stabilities for the three repillared clays are observed from the XRD patterns, surface area, and micropore volume measurements. The difference may be due to the different pillars formed from the different polyoxycations. As in studies of intercalated clays, the $GaAl_{12}$/B−H polyoxycation has the most stable Keggin structure among the three polyoxycations, so it forms the most stable Baker−Figgis ϵ isomer[32] of the Keggin structure.[33] This is also the case for repillared clays. Repillared $GaAl_{12}$/$GaAl_{12}$/B−H clay has the highest (001) peak intensity, surface area, and micropore volume, indicating the highest thermal stability even though it was heated at 700 °C for 2 h. The lower surface areas and micropore volumes for repillared clays such as Ga_{13}/$GaAl_{12}$/B−H and Al_{13}/$GaAl_{12}$/B−H (especially the latter) may be due to the sintering of pillars at high temperature. The collapsed Al_{13} pillars block N_2 molecules, which are used in surface and pore size measurements, from reaching the interlamellar spacings.

A reviewer has pointed out the marked differences in DSC of the Ga_{13}/$GaAl_{12}$/B−H and Ga^{3+}/$GaAl_{12}$/B−H samples as compared to $GaAl_{12}$/$GaAl_{12}$/B−H and Al_{13}/$GaAl_{12}$/B−H materials. The two latter samples show relatively featureless but similar DSC curves. The former two samples both have unusual DSC curves especially between 200 and 300 °C. The Ga_{13}/$GaAl_{12}$/B−H and Ga^{3+}/$GaAl_{12}$/B−H materials both have the highest [Ga] which may govern these specific transitions. Perhaps these transitions are related to the microenvironments of Ga^{3+} (perhaps extent of hydroly-

(32) Baker, L. C. W.; Figgis, J. S. *J. Am. Chem. Soc.* **1970**, *92*, 3794.
(33) (a) Keggin, J. F. *Nature* **1933**, *131*, 908. (b) Pope, M. T. *Heteropoly and Isopoly Oxometalates*; Springer-Verlag: New York, 1983; p 27.

sis). In any event, the DSC data clearly show that all four materials are unique. The $Ga^{3+}/GaAl_{12}/B-H$ sample also has a more intense peak near 450 °C than all the other samples which may also be related to it having the highest Ga content and perhaps highest degree of hydrolysis.

D. Acidicity. It is widely recognized that hydrolytic reactions of the following type generate Brønsted acid sites:

$$[M_{13}O_4(OH)_{24}(H_2O)_{12}]^{7+} \rightarrow [M_{13}O_4(OH)_{24+x}(H_2O)_{12-x}]^{(7-x)+} + xH^+$$

The Brønsted acid sites are formed at the pillar clay layer linkages in the interlamellar region. This means that more pillars can generate more acid sites on pillaring. This is also the case for repillaring. After being repillared, the acid sites are increased. Among the three repillared clays, $GaAl_{12}/GaAl_{12}/B-H$ has the largest amount of acid sites. This result is consistent with structural information that $GaAl_{12}/GaAl_{12}/B-H$ has the best pillared structure and the largest amount of pillars. Therefore, it should have the largest amount of acid sites.

The loss of some acid sites on Ga^{3+} ion-exchanged $GaAl_{12}/B-H$ is understandable. Ga^{3+} cations do not form new pillars; insteady they occupy some Brønsted sites and prevent NH_3 and pyridine molecules from being adsorbed on acid sites.

On the repillared clays, the amount of Lewis acid sites is larger than that of Brønsted acid sites. The IR bands of Lewis sites are still apparent at 550 °C. However, the bands for Brønsted sites are very weak. Readsorption of pyridine at 150 °C shows that most Lewis acid sites still exist, even after evacuation at 550 °C. Lewis sites are associated with the pillars themselves. More pillaring will therefore enhance such Lewis sites.

Of the three repillared clays, the one repillared with Ga_{13} agent has higher Brønsted/Lewis acid site ratios, especially when the samples are evacuated at higher temperatures. This result is the same as that observed earlier,[21] in which $Ga_{13}/B-H$ pillared clay is observed to have more Brønsted acid sites than the other two pillared clays. It seems that pillars generated from gallium polyoxycations produce more Brønsted acid sites than those generated from aluminum polyoxycations. This assumption may be supported by the IR data that show that acidic OH groups, introduced during pillaring, (whose bands are around 3737 cm^{-1}) of $Ga_{13}/GaAl_{12}/B-H$, are totally bonded with pyridine, while on $Al_{13}/GaAl_{12}/B-H$, some of them are still free.

Conclusions

Ammonia treatment promotes decomposition of $[GaO_4Al_{12}(OH)_{24}(H_2O)_{12}]^{7+}$ to oxide pillars and consequently produces pillared clays with a large number of cation-exchangeable sites. Reintercalation of pillared clays introduces into the pillared clay an additional number of pillars. It is apparent from the results that the polyoxycations have access to the cation-exchangeable sites on the pillared clay, although diffusional limitations appear in reintercalation. As compared to $GaAl_{12}/B-H$ before repillaring, the thermal stability of repillared clay materials has been increased, especially for $GaAl_{12}/GaAl_{12}/B-H$ and $Ga_{13}/GaAl_{12}/B-H$. The repillared clay with $GaAl_{12}$ polyoxycations has the highest thermal stability. The additional pillars introduced by repillaring gives such pillared clay materials more acid sites, especially in the case of $GaAl_{12}/GaAl_{12}/B-H$ where about 26% more acid sites are produced. However, the Ga^{3+} ion-exchanged pillared clay has less acid sites than $GaAl_{12}/B-H$. As was the case for the three pillared clays, the amount of Lewis acid sites probed by FTIR larger than Brønsted acid sites for repillared clay materials. The number of Brønsted acid sites on Ga_{13} repillared clay probed by pyridine chemisorption is greater than those on the other two repillared clays. A reviewer has pointed out that evacuation at 550 °C simply removes pyridine adsorbate and not the acid sites. Lewis sites are known to persist to temperatures of 900 °C and Brønsted sites to at least 650 °C in such materials.

Acknowledgment. We gratefully acknowledge support of this research through the National Science Foundation under Grant CBT8814974.

CM940329H